

# Engaging Alkenes in Metallaphotoredox: A Triple Catalytic, Radical Sorting Approach to Olefin-Alcohol Cross-Coupling

Qinyan Cai,<sup>‡</sup> Iona M. McWhinnie,<sup>‡</sup> Nathan W. Dow,<sup>‡</sup> Amy Y. Chan, and David W. C. MacMillan\*



Cite This: *J. Am. Chem. Soc.* 2024, 146, 12300–12309



Read Online

ACCESS |



Metrics & More



Article Recommendations



Supporting Information

**ABSTRACT:** Metallaphotoredox cross-coupling is a well-established strategy for generating clinically privileged aliphatic scaffolds via single-electron reactivity. Correspondingly, expanding metallaphotoredox to encompass new C(*sp*<sup>3</sup>)-coupling partners could provide entry to a novel, medicinally relevant chemical space. In particular, alkenes are abundant, bench-stable, and capable of versatile C(*sp*<sup>3</sup>)-radical reactivity via metal-hydride hydrogen atom transfer (MHAT), although metallaphotoredox methodologies invoking this strategy remain underdeveloped. Importantly, merging MHAT activation with metallaphotoredox could enable the cross-coupling of olefins with feedstock partners such as alcohols, which undergo facile open-shell activation via photocatalysis. Herein, we report the first C(*sp*<sup>3</sup>)-C(*sp*<sup>3</sup>) coupling of MHAT-activated alkenes with alcohols by performing deoxygenative hydroalkylation via triple cocatalysis. Through synergistic Ir photoredox, Mn MHAT, and Ni radical sorting pathways, this branch-selective protocol pairs diverse olefins and methanol or primary alcohols with remarkable functional group tolerance to enable the rapid construction of complex aliphatic frameworks.

Within organic synthesis, cross-coupling technologies have profoundly streamlined the preparation of complex, high-value molecules across numerous chemical industries.<sup>1</sup> Notably, metallaphotoredox cross-coupling harnesses reactive radical intermediates under mild, transition-metal-mediated bond-forming conditions.<sup>2</sup> By enabling open-shell functionalization of abundant feedstocks, such as amines, carboxylic acids, and C–H nucleophiles, metallaphotoredox catalysis allows fragment couplings that would be unachievable via traditional two-electron pathways.<sup>3–6</sup> These transformations are particularly suited for delivering C(*sp*<sup>3</sup>)-rich scaffolds, molecular cores increasingly recognized as vital components of clinically successful small molecule drug candidates (Figure 1a).<sup>7,8</sup> Novel metallaphotoredox methods, particularly those employing new aliphatic partners and allowing previously untenable retrosynthetic disconnections, have the potential to provide access to unexplored, medicinally relevant chemical space.<sup>9</sup>

To this end, a central goal in metallaphotoredox has been the incorporation of underutilized yet advantageous C(*sp*<sup>3</sup>)-radical progenitors within open-shell cross-coupling systems.<sup>2</sup> Among many possibilities, our laboratory recently identified olefins as a nontraditional motif that might be activated for metallaphotoredox fragment couplings. Alkenes, which are naturally occurring or readily accessible from ubiquitous precursors (e.g., halides, alcohols, carbonyls),<sup>10</sup> represent a structurally varied, bench-stable substrate class that is highly commercially available compared to traditional electrophilic and organometallic reagents (Figure 1b).<sup>11</sup> However, beyond their deployment as “conjunctive” linchpins for specific multicomponent reactions, olefins have seen limited consideration as partners for directing group-free, C(*sp*<sup>3</sup>)-enriching metallaphotoredox couplings.<sup>12,13</sup> If simpler alkene-to-C(*sp*<sup>3</sup>)-radical activation modes (primarily those more reminiscent of “conventional” cross-coupling logic)<sup>14</sup> could be employed in metallaphotoredox, pharmaceuti-

cally valuable linkages such as C–C bonds could be delivered through predictable and expedient synthetic routes. Moreover, by pairing olefins with other photoredox-compatible feedstock substrates, a range of convenient but otherwise inaccessible C(*sp*<sup>3</sup>)-C(*sp*<sup>3</sup>) fragment couplings may be realized under mild conditions.<sup>3</sup> Specifically, an alkene might be induced to undergo metallaphotoredox cross-coupling with a transient radical species derived from an alcohol substrate. To this end, we have developed an *N*-heterocyclic carbene (NHC)-mediated alcohol deoxygenation platform that can be harnessed for the direct C(*sp*<sup>3</sup>)-C(*sp*<sup>3</sup>) coupling of alcohols with acid or halide partners.<sup>13a,15,16</sup> In light of the structural variance and commercial abundance of alcohols,<sup>11</sup> we expect that a direct alcohol–alkene cross-coupling could permit single-step exploration of vast aliphatic chemical diversity.

Given that olefin  $\pi$ -systems can furnish *sp*<sup>3</sup>-based radical intermediates through various open-shell pathways, it was necessary to devise an appropriate alkene-to-radical activation strategy at the outset. Metal-hydride hydrogen atom transfer (MHAT) is capable of generating radicals via simple C–H bond-forming events and thus represents a chemoselective and retrosynthetically appealing approach to Markovnikov-selective radical production from unactivated olefins.<sup>17</sup> Using sustainable metals—such as Co, Fe, and Mn—MHAT hydrofunctionalization catalysis has enabled Mukaiyama hydrations, Giese additions, azidations, aminations, and even olefin-based cross-

Received: February 15, 2024

Revised: April 4, 2024

Accepted: April 5, 2024

Published: April 24, 2024



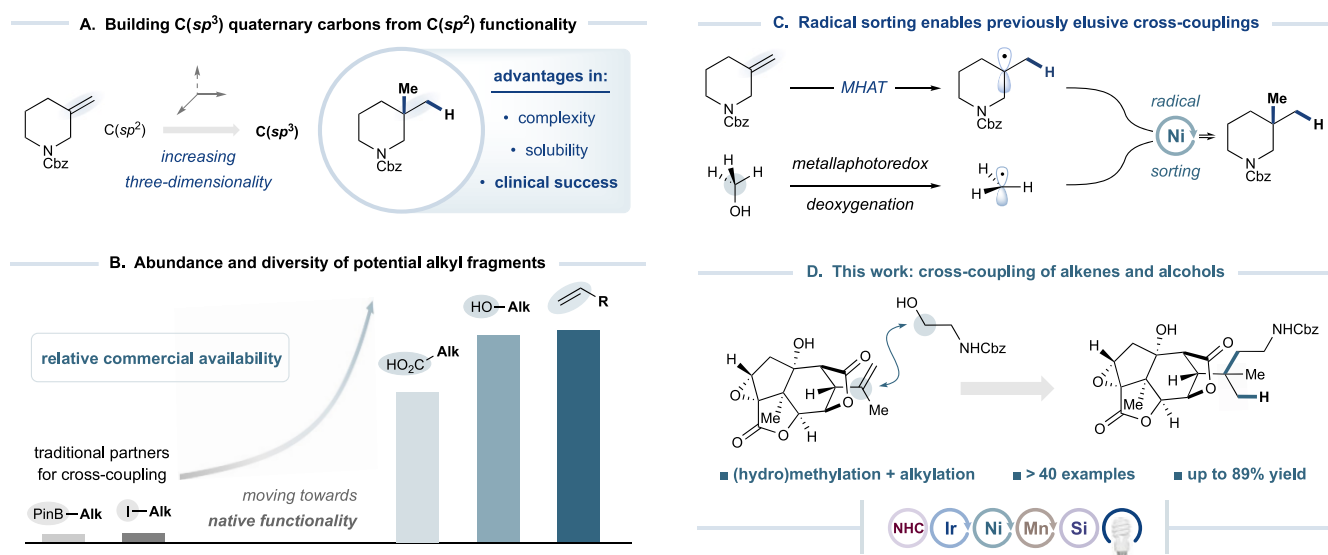


Figure 1. Metallaphotoredox olefin-alcohol cross-coupling.

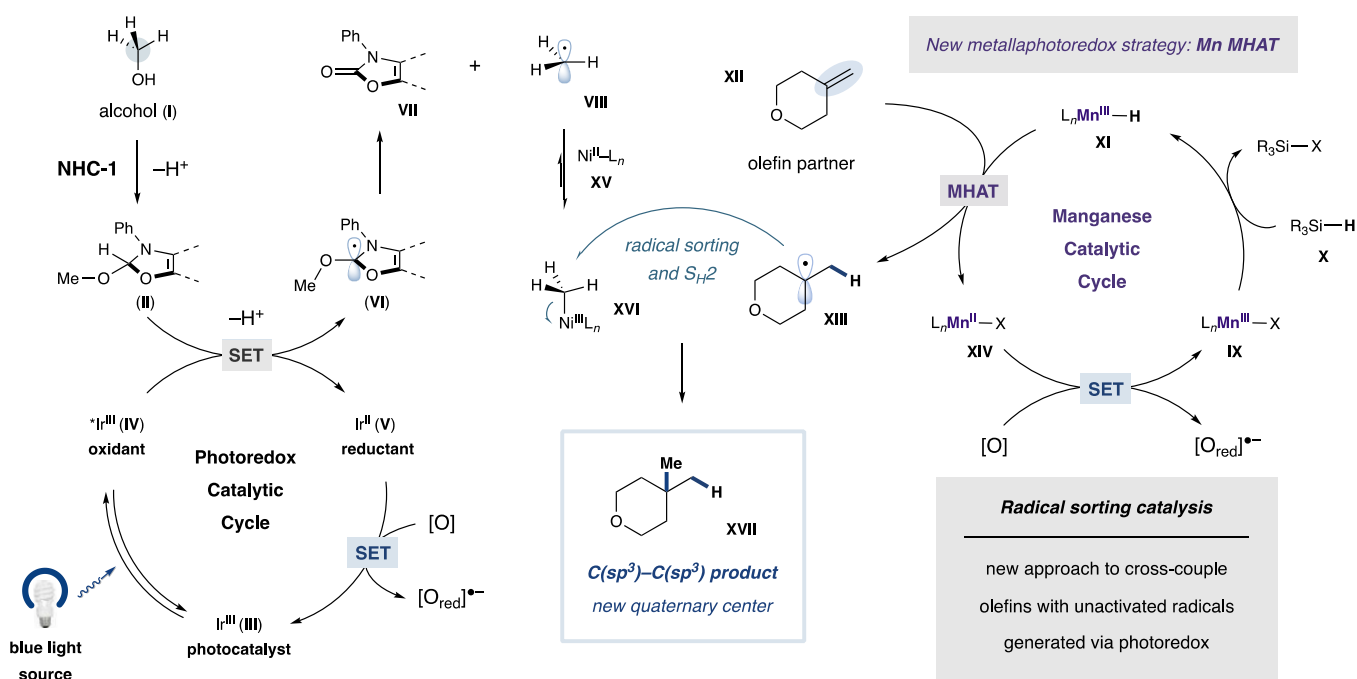


Figure 2. Plausible mechanism for olefin-alcohol cross-coupling.

couplings under thermal activation.<sup>18,19</sup> Drawing from these precedents, we proposed achieving the envisioned alkene-alcohol cross-coupling by merging MHAT-based alkene activation with NHC-mediated alcohol deoxygenation (Figure 1c).<sup>15</sup> However, the success of such a method would require hindered secondary and tertiary radicals, accessed via MHAT from common olefin substitution patterns, to undergo facile bond formation with alcohol-derived unstabilized radicals. Despite numerous advances in MHAT reactivity,<sup>17</sup> this specific type of dual radical cross-coupling has remained underdeveloped,<sup>20</sup> consistent with energetic challenges for inner-sphere reductive elimination at metal centers when using hindered radical partners.<sup>21,22</sup>

To achieve selective open-shell cross-coupling of alcohols and olefins (Figure 1d), we sought to leverage “radical sorting” catalysis, which has been recently deployed in our laboratory and

others.<sup>15b,f,23–25</sup> Under this biomimetic strategy, two carbon-centered radicals with differing substitution patterns are thermodynamically distinguished by a high-valent metal catalyst, wherein the less substituted methyl or primary radicals are preferentially captured by the metal center.<sup>24b</sup> The remaining transient nucleophilic (often tertiary) radicals can engage in *outer-sphere* bond-forming processes with the nascent and persistent electrophilic metal-alkyl intermediate.<sup>26,27</sup> Following bimolecular homolytic substitution (S<sub>H</sub>2) principles,<sup>25</sup> these events readily furnish congested motifs, including quaternary centers, while achieving cross-selectivity via “radical sorting” as dictated by metal-binding favorability and S<sub>H</sub>2 kinetics.<sup>23</sup> While related Fe-mediated MHAT couplings are known in thermal contexts,<sup>20</sup> our success in pairing unstabilized radicals via Ni(scorpionate),<sup>13,24</sup> Ni(diketonate),<sup>15b</sup> and Fe-(porphyrin)<sup>15f,23</sup> sorting platforms suggested that metallapho-

toredox could be remarkably adaptable to radical sorting with olefins and alcohols. Importantly, the synergistic use of photoredox, MHAT, and radical sorting strategies would mandate careful, coordinated optimization of each catalytic cycle, a requirement made less burdensome by the plethora of sorting catalysts available within metallaphotoredox settings.<sup>2,23–25</sup> Herein, we report a successful platform for olefin–alcohol coupling—formally a “deoxygenative hydroalkylation”—based on this mechanistic blueprint that expediently delivers C(sp<sup>3</sup>)-complexity through the coordinated action of Ir/Mn/Ni triple cocatalysis under photonic activation.

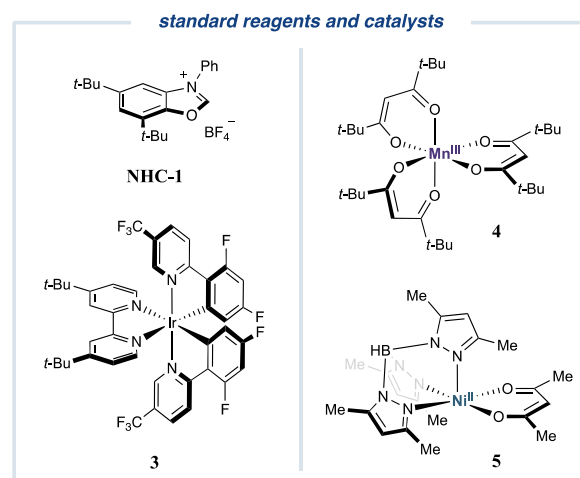
Figure 2 details a plausible olefin–alcohol cross-coupling mechanism that merges (a) NHC-mediated alcohol activation, (b) MHAT-based olefin activation, and (c) radical sorting for heteroselective bond formation. Prior to irradiation, an alcohol substrate (i.e., methanol, **1**) first condenses with a benzoxazolium salt (termed “NHC-1”) to form activated NHC–alcohol adduct **II**.<sup>15</sup> Subsequently, excitation and intersystem crossing of a suitable Ir(III) photocatalyst (**III**) under blue light irradiation could generate a long-lived and oxidizing triplet excited state **IV**.<sup>28</sup> As established previously,<sup>15</sup> adduct **II** can initiate reductive quenching with **IV** via single-electron transfer (SET), which provides reduced Ir(II) photocatalyst **V** and, after deprotonation, carbon-centered radical **VI**. Critically, this unique intermediate undergoes facile  $\beta$ -scission and liberation of both a stable carbamate byproduct (**VII**) and the desired methyl radical (**VIII**). Concurrently, transmetalation between Mn(III) MHAT (pre)catalyst **IX** and hydrosilane reagent **X** affords Mn–H intermediate **XI**.<sup>17</sup> Ensuing MHAT between **XI** and olefin **XII** would furnish tertiary radical **XIII** and the Mn(II) intermediate **XIV**. With reduced forms of the photocatalyst and MHAT catalyst now present, we anticipated that mild exogenous oxidants could promote SET events that regenerate both ground-state Ir(III) photocatalyst **III** and starting MHAT catalyst **IX**.<sup>29,30</sup> Lastly, in the crucial coupling event between radicals **VIII** and **XIII**, Ni(II) sorting catalyst **XV** would preferentially capture the less substituted methyl radical, thereby delivering persistent Ni(III)–methyl species **XVI**. Free tertiary radical **XIII** could then undergo S<sub>H</sub>2 displacement with complex **XVI**,<sup>23–25</sup> affording C(sp<sup>3</sup>)-C(sp<sup>3</sup>) cross-coupled product **XVII** while regenerating Ni catalyst **XV**.<sup>31</sup>

Recognizing the importance of the “magic methyl effect” in pharmaceutical design, we first evaluated our proposed olefin–alcohol coupling for deoxygenative hydromethylation using alkene **1** and methanol as a widely available yet nontraditional methylating agent (Table 1; see Supporting Information (SI) for details).<sup>32</sup> Delightfully, quaternary product **2** was obtained in 75% yield using Ir[dF(CF<sub>3</sub>)ppy]<sub>2</sub>(dtbbpy)PF<sub>6</sub> (**3**;  $\tau = 2.3 \mu\text{s}$ ;  $E_{1/2}^{\text{red}}[\text{*Ir}^{\text{III}}/\text{Ir}^{\text{II}}] = +1.21 \text{ V vs SCE in MeCN}$ )<sup>28</sup> as a photocatalyst under standardized 450 nm Integrated Photo-reactor (IPR) irradiation (entry 1).<sup>33</sup> These optimal conditions also featured hydrosilane reagent 1,1,3,3-tetramethyldisiloxane (TMDS), benzoyl peroxide as a mild oxidant, Mn(dpm)<sub>3</sub> (**4**, dpm = dipivaloylmethane) for MHAT activation, and Ni-scorpionate catalyst **5** (formed *in situ* from Ni(acac)<sub>2</sub> and trispyrazolylborate ligand KTp\*)<sup>24</sup> for radical sorting (Figure 2), alongside beneficial base and water additives (entries 2 and 3).<sup>34</sup> As outlined in Table 1, judicious catalyst selection proved essential for reactivity.<sup>2,17</sup> For the radical sorting step, product **2** was obtained in minimal yield using Fe-based catalysts<sup>15f,20,23</sup> or in the absence of sorting conditions (entries 4 and 5). By contrast, diketone- and KTp\*-ligated Ni complexes—which are known to promote radical sorting reactivity—were each

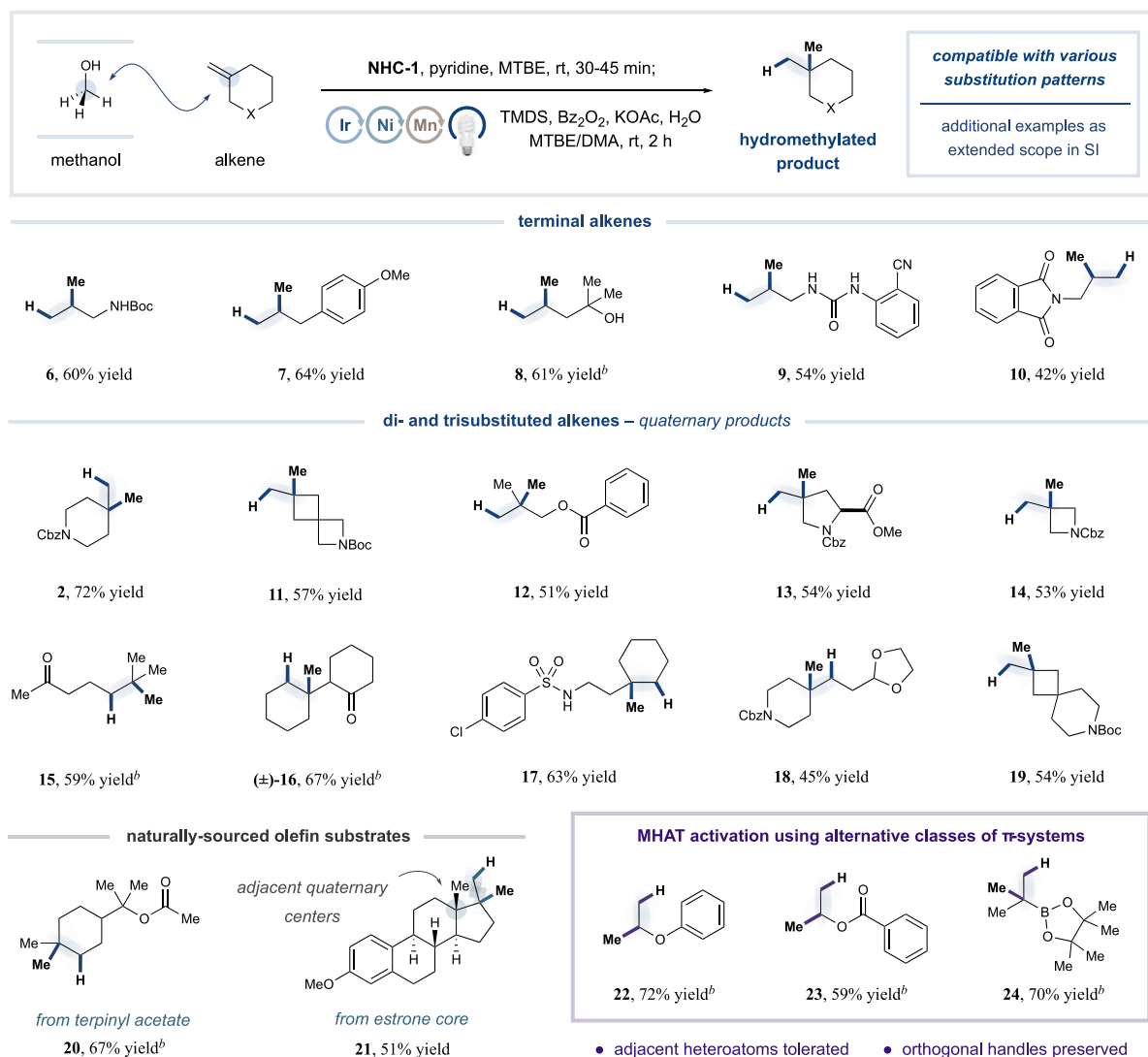
Table 1. Optimization and Control Reactions<sup>a</sup>

| entry | deviation  | yield <sup>b</sup> |
|-------|--|--------------------|
| 1     | none   | 75%                |
| 2     | in absence of base (KOAc)                              | 65%                |
| 3     | in absence of H <sub>2</sub> O additive                | 65%                |
| 4     | Fe(OEP)Cl instead of <b>5</b>                          | 2%                 |
| 5     | no Ni catalyst <b>5</b>                                | 10%                |
| 6     | Ni(acac) <sub>2</sub> instead of <b>5</b>              | 67%                |
| 7     | Fe(acac) <sub>3</sub> instead of <b>4</b>              | 9%                 |
| 8     | Co(acac) <sub>2</sub> or Co(salen) instead of <b>4</b> | 4%                 |
| 9     | no Mn catalyst <b>4</b>                                | 0%                 |
| 10    | no light   | 5%                 |
| 11    | no photocatalyst <b>3</b>                              | 19%                |
| 12    | no TMDS  | 0%                 |
| 13    | no oxidant   | 0%                 |

<sup>a</sup>Typically performed with 0.5 equiv. KOAc, 5 equiv. H<sub>2</sub>O and 4:1 MTBE/DMA. See SI for experimental details. <sup>b</sup>Yield determined by <sup>1</sup>H NMR. Ac, acetyl; Acac, acetylacetonate; Bz, benzoyl; Cbz, benzyloxycarbonyl; DMA, N,N-dimethylacetamide; MTBE, methyl *tert*-butyl ether; OEP, 2,3,7,8,12,13,17,18-octaethyl-21H,23H-porphine.



effective in some capacity (entry 6).<sup>15b,24</sup> Moreover, Mn-catalyzed olefin activation emerged as a privileged option over Fe–H, Co–H, and MHAT-free systems (entries 7–9).<sup>17</sup> When considering the various Mn, Fe and Co complexes suitable for MHAT, different catalysts may show distinct thermodynamic capacities to compete with Ni for methyl radical capture,<sup>35</sup> behavior consistent with open-shell formation of metal–alkyl intermediates in previous MHAT systems.<sup>36</sup> Beyond differences in redox potentials, we hypothesize that the chosen Mn catalyst effectively avoids radical capture and off-cycle Mn–methyl formation, instead favoring productive Mn(III)–H activity.<sup>17,35</sup> These unique advantages of synergistic Ir/Mn/Ni triple catalysis for olefin activation and radical sorting are an emerging topic that will be addressed in subsequent studies.<sup>31</sup> Lastly, additional control reactions demonstrated that blue light, photocatalyst, hydrosilane, and oxidant were required for sufficient reactivity (entries 10–13), consistent with the metallaphotoredox–MHAT mechanistic blueprint outlined in Figure 2.<sup>37,38</sup>

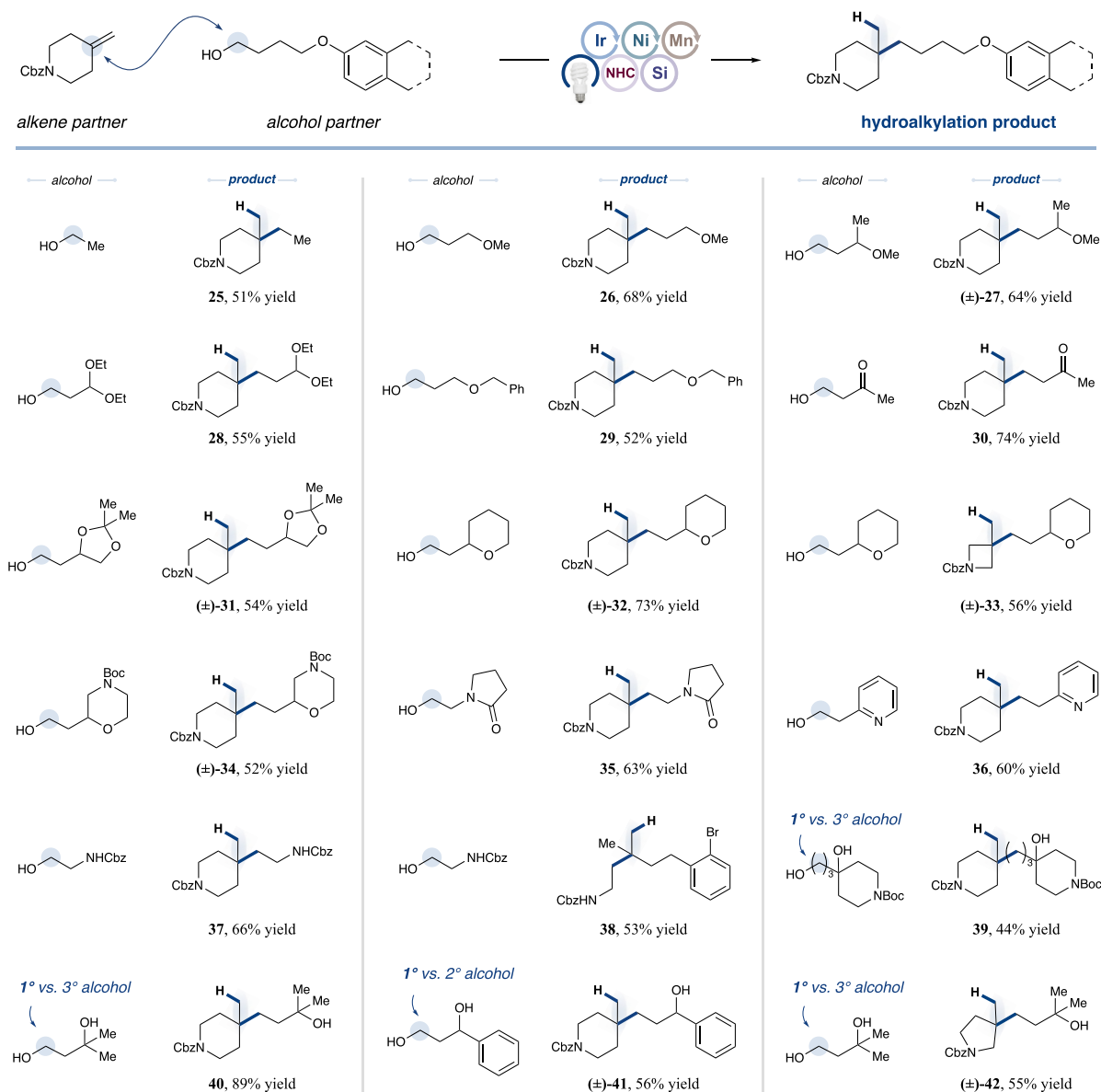
Table 2. Alkene Scope for Methanol-Enabled Hydromethylation<sup>a</sup>

<sup>a</sup>Typically performed using methanol (3 equiv), NHC-1 (3.3 equiv), pyridine (3.15 equiv) in MTBE (0.50 M) for 30–45 min, then alkene (0.5 mmol, 1 equiv), **3** (0.25 mol %), **4** (20 mol %), **5** (10 mol %), TMS (5 equiv), Bz<sub>2</sub>O<sub>2</sub> (4 equiv), KOAc (0.5 equiv), H<sub>2</sub>O (5 equiv) and MTBE/DMA (4:1, 0.067 M), under IPR irradiation (450 nm) for 2 h. All yields isolated unless noted otherwise. See SI for experimental details. <sup>b</sup>Yield determined by <sup>1</sup>H NMR (due to volatility/instability). Boc, *tert*-butoxycarbonyl.

With optimal conditions in hand, we next evaluated the alkene scope for this transformation. To our delight, Markovnikov hydromethylation was achievable with a full branched selectivity across a range of alkene substitution patterns (Table 2). Notably, while terminal olefins furnish modestly nucleophilic secondary radicals upon MHAT activation,<sup>17,26</sup> these intermediates consistently underwent facile radical sorting to deliver hydromethylated products (**6–10**, 42–64% yield). Additionally, substrates bearing hindered di- or trisubstituted alkenes were readily leveraged as tertiary radical precursors via MHAT. This extension resulted in products containing quaternary centers (**2** and **11–19**, 45–72% yield), motifs that remain elusive under many typical cross-coupling conditions.<sup>21,22</sup> Given the absence of low-valent Ni intermediates (e.g., Ni(0) species) in Ni(II)/Ni(III) radical sorting platforms,<sup>15b,24</sup> a selection of functional groups typically sensitive to oxidative addition, including allylic carboxylates and aryl halides, are chemoselectively tolerated in all cases.<sup>39</sup> Moreover, several naturally sourced terpenoid- and hormone-derived substrates were

competent within this protocol (**20** and **21**, 67% and 51% yield, respectively), furnishing congested motifs (including contiguous quaternary carbons) in short order. Beyond traditional “unactivated” alkenes, deoxygenative hydromethylation could be extended to heteroatom-bearing  $\pi$ -partners (**22–24**, 59–72% yield), a finding that may inform C(*sp*<sup>3</sup>)-enriching coupling sequences via exploitation of retained orthogonal functionality (i.e., boronic esters).<sup>40</sup> Overall, this protocol affords medicinally valuable gem-dimethyl, methylcycloalkyl, and quaternary units from diverse olefins,<sup>41</sup> all while using a bulk solvent (methanol) as an atypical methylating reagent.<sup>42</sup>

To probe the versatility of this new technology, we next investigated the scope of alcohols amenable to deoxygenative hydroalkylation (Table 3). Using Ni(diketonate) sorting catalysts,<sup>15b</sup> an array of primary substrates were readily paired with hindered olefins to provide direct access to quaternary centers (see SI for additional hydroalkylation examples).<sup>42</sup> Gratifyingly, ethanol and ether-, acetal-, or ketone-containing alcohol substrates were broadly successful (**25–31**, 51–74%

Table 3. Alcohol Scope for Deoxygenative Hydroalkylation<sup>a</sup>

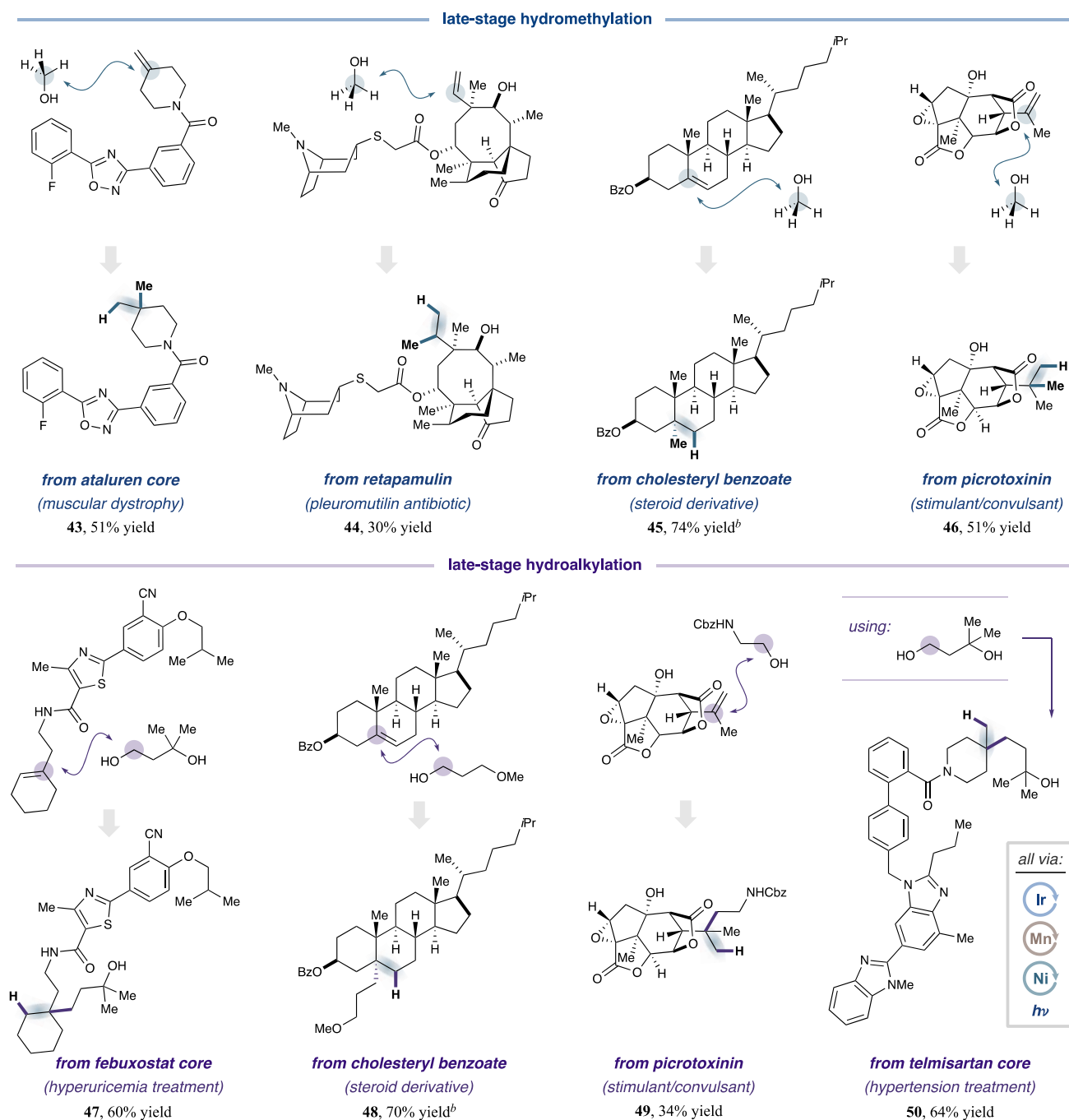
<sup>a</sup>Isolated yields reported. See SI for experimental details.

yield), as were substrates bearing tetrahydropyran (**32** and **33**, 73% and 56% yield, respectively), morpholine (**34**, 52% yield), lactam (**35**, 63% yield), or pyridine (**36**, 60% yield) heterocyclic functionality. Moreover, the functional group tolerance of this method allowed for retention of protic motifs, such as amine derivatives and unprotected distal alcohols (**37–42**, 44–89% yield). This finding is significant given that sequential, site-selective diol deoxygenations are well-established using NHC-1;<sup>15</sup> as such, MHAT-olefin coupling may represent a practical entry point toward elaborating native polyols into complex alkylated scaffolds.

Lastly, to rapidly produce drug-like molecular architecture from native functionality,<sup>7–9</sup> we harnessed olefin–alcohol coupling for the late-stage derivatization of therapeutic scaffolds. Using a selection of commercial alcohols, diverse C(sp<sup>3</sup>)-rich products were furnished directly from bioactive compounds bearing pendant olefins (Table 4). Through the hydroalkylation of antibiotics, antihypertensives, stimulants, steroids, and

muscular dystrophy or hyperuricemia medications, this approach delivered a series of novel and potentially efficacious drug analogues amenable to further evaluation (**43–50**, 30–74% yield). Across all cases, the unique tolerance of this method for labile functionality—including epoxides, oxidation-sensitive amines or sulfides, coordinating alcohols or heteroarenes, and oxidative addition-prone 1,2,4-oxadiazoles<sup>4a,43–45</sup>—was critical for generating complex molecular architecture efficiently.

Collectively, these examples underscore the utility, expediency, and selectivity offered by metallaphotoredox olefin–alcohol coupling in the construction of aliphatic scaffolds of medicinal relevance. Moreover, we envision that synergistic Ir/Mn/Ni triple cocatalysis can be generically advantageous for C(sp<sup>3</sup>)-C(sp<sup>3</sup>) bond formations between olefins and various radical partners. As such, further mechanistic evaluation and application of this photocatalytic platform will be reported in due course.

Table 4. Hydroalkylation of Bioactive Compounds<sup>a</sup>

<sup>a</sup>All yields isolated unless noted otherwise. See SI for experimental details. <sup>b</sup>Yield determined by <sup>1</sup>H NMR.

## ASSOCIATED CONTENT

### Supporting Information

The Supporting Information is available free of charge at <https://pubs.acs.org/doi/10.1021/jacs.4c02316>.

Experimental details, expanded substrate table, compound characterization data, and spectra (PDF)

## AUTHOR INFORMATION

### Corresponding Author

David W. C. MacMillan – Merck Center for Catalysis at Princeton University, Princeton, New Jersey 08544, United

States; [orcid.org/0000-0001-6447-0587](https://orcid.org/0000-0001-6447-0587);  
Email: [dmacmill@princeton.edu](mailto:dmacmill@princeton.edu)

### Authors

Qinyan Cai – Merck Center for Catalysis at Princeton University, Princeton, New Jersey 08544, United States;  
[orcid.org/0000-0002-5908-2560](https://orcid.org/0000-0002-5908-2560)

Iona M. McWhinnie – Merck Center for Catalysis at Princeton University, Princeton, New Jersey 08544, United States

Nathan W. Dow – Merck Center for Catalysis at Princeton University, Princeton, New Jersey 08544, United States;  
[orcid.org/0000-0003-1071-0201](https://orcid.org/0000-0003-1071-0201)

Amy Y. Chan – Merck Center for Catalysis at Princeton University, Princeton, New Jersey 08544, United States; [orcid.org/0009-0002-6492-5873](https://orcid.org/0009-0002-6492-5873)

Complete contact information is available at: <https://pubs.acs.org/10.1021/jacs.4c02316>

### Author Contributions

<sup>‡</sup>Q.C., I.M.M., and N.W.D. contributed equally.

### Notes

The authors declare the following competing financial interest(s): D.W.C.M. declares a competing financial interest with respect to the Integrated Photoreactor.

### ACKNOWLEDGMENTS

The authors are grateful for financial support provided by the National Institute of General Medical Sciences (NIGMS) of the National Institutes of Health (R35GM134897-05); BioLEC, an Energy Frontier Research Center (US Department of Energy, Office of Science, Office of Basic Energy Sciences, under award DE-SC0019370); the Princeton Catalysis Initiative; and kind gifts from Merck, Janssen, Bristol-Myers Squibb, Genentech, Genmab, and Pfizer. The content is solely the responsibility of the authors and does not necessarily represent the official views of NIGMS. Q.C. and I.M.M. acknowledge Princeton University for financial support through a first-year graduate fellowship. The authors thank Christina Kraml, Neal Byrne, and Dr. Yingru Zhang (Lotus Separations) for assistance with compound purification; Ken Conover and Dr. István Pelczer for NMR support; Dr. John Eng for mass spectroscopy support; Dr. Niels Bisballe, Dr. Benjamin Boyle, Dr. Colin Gould, Nicholas Intermaggio, Cesar Nicolas Prieto-Kullmer, Dr. James Rossi-Ashton, Dr. Holt Sakai, Dr. Artem Tsybmal, and Dr. Jiaxin Xie for helpful scientific discussions; and Rebecca Lambert for assistance with the preparation and editing of this manuscript.

### REFERENCES

- (1) (a) Campeau, L. C.; Hazari, N. Cross-Coupling and Related Reactions: Connecting Past Success to the Development of New Reactions for the Future. *Organometallics* **2019**, *38*, 3–35. (b) Buskes, M. J.; Blanco, M.-J. Impact of Cross-Coupling Reactions in Drug Discovery and Development. *Molecules* **2020**, *25*, 3493–3514.
- (2) Chan, A. Y.; Perry, I. B.; Bissonnette, N. B.; Buksh, B. F.; Edwards, G. A.; Frye, L. I.; Garry, O. L.; Lavagnino, M. N.; Li, B. X.; Liang, Y.; et al. Metallaphotoredox: The Merger of Photoredox and Transition Metal Catalysis. *Chem. Rev.* **2022**, *122*, 1485–1542.
- (3) For general reviews addressing (metalla)photoredox activation and its applicability towards conventionally inert functional groups, see: (a) Studer, A.; Curran, D. P. Catalysis of Radical Reactions: a Radical Chemistry Perspective. *Angew. Chem., Int. Ed.* **2016**, *55*, 58–102. (b) Matsui, J. K.; Lang, S. B.; Heitz, D. R.; Molander, G. A. Photoredox-Mediated Routes to Radicals: The Value of Catalytic Radical Generation in Synthetic Methods Development. *ACS Catal.* **2017**, *7*, 2563–2575. (c) Schwarz, J.; König, B. Decarboxylative Reactions With and Without Light – A Comparison. *Green Chem.* **2018**, *20*, 323–361. (d) Crespi, S.; Fagnoni, M. Generation of Alkyl Radicals: From the Tyranny of Tin to the Photon Democracy. *Chem. Rev.* **2020**, *120*, 9790–9833. (e) Holmberg-Douglas, N.; Nicewicz, D. A. Photoredox-Catalyzed C–H Functionalization Reactions. *Chem. Rev.* **2022**, *122*, 1925–2016.
- (4) For representative examples of open-shell amine activation via (metalla)photoredox, see: (a) Beatty, J. W.; Stephenson, C. R. J. Amine Functionalization via Oxidative Photoredox Catalysis: Methodology Development and Complex Molecule Synthesis. *Acc. Chem. Res.* **2015**, *48*, 1474–1484. (b) Correia, J. T. M.; Fernandes, V. A.; Matsuo, B. T.; Delgado, J. A. C.; de Souza, W. C.; Paixão, M. W. Photoinduced Deaminative Strategies: Katritzky Salts as Alkyl Radical Precursors. *Chem. Commun.* **2020**, *56*, 503–514. (c) Ashley, M. A.; Rovis, T. Photoredox-Catalyzed Deaminative Alkylation via C–N Bond Activation of Primary Amines. *J. Am. Chem. Soc.* **2020**, *142*, 18310–18316.
- (5) For representative examples of open-shell carboxylic acid activation via (metalla)photoredox, see: (a) Zuo, Z.; MacMillan, D. W. C. Decarboxylative Arylation of  $\alpha$ -Amino Acids via Photoredox Catalysis: A One-Step Conversion of Biomass to Drug Pharmacophore. *J. Am. Chem. Soc.* **2014**, *136*, 5257–5260. (b) Schwarz, J.; König, B. Decarboxylative Reactions With and Without Light – A Comparison. *Green Chem.* **2018**, *20*, 323–361. (c) Beil, S. B.; Chen, T. Q.; Intermaggio, N. E.; MacMillan, D. W. C. Carboxylic Acids as Adaptive Functional Groups in Metallaphotoredox Catalysis. *Acc. Chem. Res.* **2022**, *55*, 3481–3494.
- (6) For representative examples of open-shell C–H nucleophile activation via (metalla)photoredox, see: (a) Tucker, J. W.; Narayanam, J. M. R.; Krabbe, S. W.; Stephenson, C. R. J. Electron Transfer Photoredox Catalysis: Intramolecular Radical Addition to Indoles and Pyrroles. *Org. Lett.* **2010**, *12*, 368–371. (b) Shi, L.; Xia, W. Photoredox Functionalization of C–H Bonds Adjacent to a Nitrogen Atom. *Chem. Soc. Rev.* **2012**, *41*, 7687–7697. (c) Xie, J.; Jin, H.; Xu, P.; Zhu, C. When C–H Bond Functionalization Meets Visible-Light Photoredox Catalysis. *Tetrahedron Lett.* **2014**, *55*, 36–48. (d) Qin, Q.; Jiang, H.; Hu, Z.; Ren, D.; Yu, S. Functionalization of C–H Bonds by Photoredox Catalysis. *Chem. Rec.* **2017**, *17*, 754–774. (e) Holmberg-Douglas, N.; Nicewicz, D. A. Photoredox-Catalyzed C–H Functionalization Reactions. *Chem. Rev.* **2022**, *122*, 1925–2016.
- (7) Singh, P. P.; Singh, P. K.; Srivastava, V. Visible Light Metallaphotoredox Catalysis in the Late-Stage Functionalization of Pharmaceutically Potent Compounds. *Org. Chem. Front.* **2022**, *10*, 216–236.
- (8) (a) Lovering, F.; Bikker, J.; Humblet, C. Escape from Flatland: Increasing Saturation as an Approach to Improving Clinical Success. *J. Med. Chem.* **2009**, *52*, 6752–6756. (b) Foley, D. J.; Craven, P. G. E.; Collins, P. M.; Doveston, R. G.; Aimon, A.; Talon, R.; Churcher, I.; von Delft, F.; Marsden, S. P.; Nelson, A. Synthesis and Demonstration of the Biological Relevance of  $sp^3$ -rich Scaffolds Distantly Related to Natural Product Frameworks. *Chem.–Eur. J.* **2017**, *23*, 15227–15232.
- (9) Cernak, T.; Dykstra, K. D.; Tyagarajan, S.; Vachal, P.; Krska, S. W. The Medicinal Chemist's Toolbox for Late Stage Functionalization of Drug-like Molecules. *Chem. Soc. Rev.* **2016**, *45*, 546–576.
- (10) Zacharopoulou, V.; Lemonidou, A. Olefins from Biomass Intermediates: A Review. *Catalysts* **2018**, *8*, 2–19.
- (11) For the purposes of this manuscript, commercial availability for each  $sp^3$ -based substrate class displayed in Figure 1 was assessed using the Reaxys database. The reported counts represent the number of compounds which can be acquired from at least one listed chemical vendor for \$500 per purchase or less (amount of material available per purchase varies). Using these criteria, substructure searches via Reaxys produced the following numbers of commercial compounds for each substrate class: aliphatic organoboron partners – 1,318; alkyl iodides – 2,365; alkyl carboxylic acids – 247,411; aliphatic alcohols – 337,265; alkenes – 346,239 (across all substitution patterns and substituent identities). Reaxys; Elsevier, n.d. <https://www.reaxys.com/#/search/quick> (accessed 2024-01-06).
- (12) For representative examples of multicomponent cross-coupling reactions that exploit preinstalled directing or stabilizing functionality within olefins, see: (a) Derosa, J.; Tran, V. T.; van der Puy, V. A.; Engle, K. M. Carbon–Carbon  $\pi$ -Bonds as Conjugative Reagents in Cross-Coupling. *Aldrichimica Acta* **2018**, *51*, 21–32. (b) Derosa, J.; Apolinar, O.; Kang, T.; Tran, V. T.; Engle, K. M. Recent Developments in Nickel-Catalyzed Intermolecular Dicarbofunctionalization of Alkenes. *Chem. Sci.* **2020**, *11*, 4287–4296. (c) Lu, F.-D.; He, G.-F.; Lu, L.-Q.; Xiao, W.-J. *Green Chem.* **2021**, *23*, 5379–5393. (d) Liu, L.; Aguilera, M. C.; Lee, W.; Youshaw, C. R.; Neidig, M. L.; Gutierrez, O. General Method for Iron-Catalyzed Multicomponent Radical Cascades–Cross-Couplings. *Science* **2021**, *374*, 432–439. (e) Zhang, J. X.; Shu, W. Ni-Catalyzed

Reductive 1,2-Cross-Dialkylation of Unactivated Alkenes with Two Alkyl Bromides. *Org. Lett.* **2022**, *24*, 3844–3849.

(13) For recent examples of directing group-free metallaphotoredox multicomponent olefin reactions that can forge typically challenging C(sp<sup>3</sup>)-C(sp<sup>3</sup>) bonds, see: (a) Wang, J. Z.; Lyon, W. L.; MacMillan, D. W. C. Alkene Dialkylation by Triple Radical Sorting. *Nature* **2024**, *628*, 104–109. (b) Cong, F.; Sun, G.-Q.; Ye, S.-H.; Hu, R.; Rao, W.; Koh, M. J. A Bimolecular Homolytic Substitution-Enabled Platform for Multicomponent Cross-Coupling of Unactivated Alkenes. *ChemRxiv* **2023**, DOI: 10.26434/chemrxiv-2023-mpqdw (accessed 2024-02-04).

(14) Smith, J. M.; Harwood, S. J.; Baran, P. S. Radical Retrosynthesis. *Acc. Chem. Res.* **2018**, *51*, 1807–1817.

(15) (a) Dong, Z.; MacMillan, D. W. C. Metallaphotoredox-Enabled Deoxygenative Arylation of Alcohols. *Nature* **2021**, *598*, 451–456. (b) Sakai, H. A.; MacMillan, D. W. C. Nontraditional Fragment Couplings of Alcohols and Carboxylic Acids: C(sp<sup>3</sup>)-C(sp<sup>3</sup>) Cross-Coupling via Radical Sorting. *J. Am. Chem. Soc.* **2022**, *144*, 6185–6192. (c) Wang, J. Z.; Sakai, H. A.; MacMillan, D. W. C. Alcohols as Alkylating Agents: Photoredox-Catalyzed Conjugate Alkylation via In Situ Deoxygenation. *Angew. Chem., Int. Ed.* **2022**, *61*, No. e202207150. (d) Intermaggio, N. E.; Millet, A.; Davis, D. L.; MacMillan, D. W. C. Deoxytrifluoromethylation of Alcohols. *J. Am. Chem. Soc.* **2022**, *144*, 11961–11968. (e) Lyon, W. L.; MacMillan, D. W. C. Expedient Access to Underexplored Chemical Space: Deoxygenative C(sp<sup>3</sup>)-C(sp<sup>3</sup>) Cross-Coupling. *J. Am. Chem. Soc.* **2023**, *145*, 7736–7742. (f) Gould, C. A.; Pace, A. L.; MacMillan, D. W. C. Rapid and Modular Access to Quaternary Carbons from Tertiary Alcohols via Bimolecular Homolytic Substitution. *J. Am. Chem. Soc.* **2023**, *145*, 16330–16336. (g) Carson, W. P., II; Sarver, P. J.; Goudy, N. S.; MacMillan, D. W. C. Photoredox Catalysis-Enabled Sulfination of Alcohols and Bromides. *J. Am. Chem. Soc.* **2023**, *145*, 20767–20774.

(16) For select examples of alternative photocatalytic strategies that can transform alcohols or related derivatives to open-shell intermediates, see: (a) Lackner, G. L.; Quasdorf, K. W.; Overman, L. E. Direct Construction of Quaternary Carbons from Tertiary Alcohols via Photoredox-Catalyzed Fragmentation of *tert*-Alkyl *N*-Phthalimidoyl Oxalates. *J. Am. Chem. Soc.* **2013**, *135*, 15342–15345. (b) Cheneberg, L.; Baralle, A.; Daniel, M.; Fensterbank, L.; Goddard, J.-P.; Ollivier, C. Visible Light Photocatalytic Reduction of *O*-Thiocarbamates: Development of a Tin-Free Barton-McCombie Deoxygenation Reaction. *Adv. Synth. Catal.* **2014**, *356*, 2756–2762. (c) Rackl, D.; Kais, V.; Kreitmeier, P.; Reiser, O. Visible Light Photoredox-Catalyzed Deoxygenation of Alcohols. *Beilstein J. Org. Chem.* **2014**, *10*, 2157–2165. (d) Vara, B. A.; Patel, N. R.; Molander, G. A. *O*-Benzyl Xanthate Esters under Ni/Photoredox Dual Catalysis: Selective Radical Generation and Csp<sup>3</sup>-Csp<sup>2</sup> Cross-Coupling. *ACS Catal.* **2017**, *7*, 3955–3959. (e) Stache, E. E.; Ertel, A. B.; Rovis, T.; Doyle, A. G. Generation of Phosphoranyl Radicals via Photoredox Catalysis Enables Voltage-Independent Activation of Strong C–O Bonds. *ACS Catal.* **2018**, *8*, 11134–11139. (f) Guo, H.-M.; Wu, X. Selective Deoxygenative Alkylation of Alcohols via Photocatalytic Domino Radical Fragmentations. *Nat. Commun.* **2021**, *12*, 5365–5374.

(17) (a) Crossley, S. W.; Obradors, C.; Martinez, R. M.; Shenvi, R. A. Mn-, Fe-, and Co-Catalyzed Radical Hydrofunctionalizations of Olefins. *Chem. Rev.* **2016**, *116*, 8912–9000. (b) Wu, J.; Ma, Z. Metal-Hydride Hydrogen Atom Transfer (MHAT) Reactions in Natural Product Synthesis. *Org. Chem. Front.* **2021**, *8*, 7050–7076.

(18) For representative examples of methodology development and application within the field of MHAT olefin hydrofunctionalization, see: (a) Feder, H. M.; Halpern, J. Mechanism of the Cobalt Carbonyl-Catalyzed Homogeneous Hydrogenation of Aromatic Hydrocarbons. *J. Am. Chem. Soc.* **1975**, *97*, 7186–7188. (b) Chung, S.-K. Selective Reduction of Mono- and Disubstituted Olefins by Sodium Borohydride and Cobalt(II). *J. Org. Chem.* **1979**, *44*, 1014–1016. (c) Isayama, S.; Mukaiyama, T. A New Method for Preparation of Alcohols from Olefins with Molecular Oxygen and Phenylsilane by the use of Bis(acetylacetonato)cobalt(II). *Chem. Lett.* **1989**, *18*, 1071–1074. (d) Mukaiyama, T.; Isayama, S.; Inoki, S.; Kato, K.; Yamada, T.; Takai, T. Oxidation-Reduction Hydration of Olefins with Molecular

Oxygen and 2-Propanol Catalyzed by Bis(acetylacetonato)cobalt(II). *Chem. Lett.* **1989**, *18*, 449–452. (e) Matsushita, Y.-i.; Matsui, T.; Sugamoto, K. Cobalt(II) Porphyrin-Catalyzed Oxidation of Olefins to Ketones with Molecular Oxygen and Triethylsilane in 2-Propanol. *Chem. Lett.* **1992**, *21*, 1381–1384. (f) Takeuchi, M.; Kano, K. (*s*-Alkyl) iron Complexes as Intermediates in (Porphinato)Iron-Mediated Reduction of Alkenes and Alkynes with Sodium Borohydride. *Organometallics* **1993**, *12*, 2059–2064. (g) Magnus, P.; Payne, A. H.; Waring, M. J.; Scott, D. A.; Lynch, V. Conversion of  $\alpha,\beta$ -Unsaturated Ketones into  $\alpha$ -Hydroxy Ketones Using an Mn<sup>III</sup> Catalyst, Phenylsilane and Dioxygen: Acceleration of Conjugate Hydride Reduction by Dioxygen. *Tetrahedron Lett.* **2000**, *41*, 9725–9730. (h) Baik, T.-G.; Luis, A. L.; Wang, L.-C.; Krische, M. J. Diastereoselective Cobalt-Catalyzed Aldol and Michael Cycloreductions. *J. Am. Chem. Soc.* **2001**, *123*, 5112–5113. (i) Shey, J.; McGinley, C. M.; McCauley, K. M.; Dearth, A. S.; Young, B. T.; van der Donk, W. A. Mechanistic Investigation of a Novel Vitamin B12-Catalyzed Carbon–Carbon Bond Forming Reaction, the Reductive Dimerization of Arylalkenes. *J. Org. Chem.* **2002**, *67*, 837–846. (j) Waser, J.; Carreira, E. M. Convenient Synthesis of Alkylhydrazides by the Cobalt-Catalyzed Hydrohydrazination Reaction of Olefins and Azodicarboxylates. *J. Am. Chem. Soc.* **2004**, *126*, 5676–5677. (k) Sato, M.; Gunji, Y.; Ikeno, T.; Yamada, T. Stereoselective Preparation of  $\alpha$ -Hydroxycarboxamide by Manganese Complex Catalyzed Hydration of  $\alpha,\beta$ -Unsaturated Carboxamide with Molecular Oxygen and Phenylsilane. *Chem. Lett.* **2004**, *33*, 1304–1305. (l) Waser, J.; Nambu, H.; Carreira, E. M. Cobalt-Catalyzed Hydroazidation of Olefins: Convenient Access to Alkyl Azides. *J. Am. Chem. Soc.* **2005**, *127*, 8294–8295. (m) Hartung, J.; Pulling, M. E.; Smith, D. M.; Yang, D. X.; Norton, J. R. Initiating Radical Cyclizations by H• Transfer from Transition Metals. *Tetrahedron* **2008**, *64*, 11822–11830. (n) Prateetongkum, S.; Jovel, I.; Jackstell, R.; Vogl, N.; Weckbecker, C.; Beller, M. First Iron-Catalyzed Synthesis of Oximes from Styrenes. *Chem. Commun.* **2009**, 1990–1992. (o) Barker, T. J.; Boger, D. L. Fe(III)/NaBH<sub>4</sub>-mediated free radical hydrofluorination of unactivated alkenes. *J. Am. Chem. Soc.* **2012**, *134*, 13588–13591. (p) Shigehisa, H.; Aoki, T.; Yamaguchi, S.; Shimizu, N.; Hiroya, K. Hydroalkoxylation of Unactivated Olefins with Carbon Radicals and Carbocation Species as Key Intermediates. *J. Am. Chem. Soc.* **2013**, *135*, 10306–10309. (q) Lo, J. C.; Yabe, Y.; Baran, P. S. A Practical and Catalytic Reductive Olefin Coupling. *J. Am. Chem. Soc.* **2014**, *136*, 1304–1307. (r) King, S. M.; Ma, X.; Herzon, S. B. A Method for the Selective Hydrogenation of Alkenyl Halides to Alkyl Halides. *J. Am. Chem. Soc.* **2014**, *136*, 6884–6887. (s) Iwasaki, K.; Wan, K. K.; Oppedisano, A.; Crossley, S. W. M.; Shenvi, R. A. Simple, Chemo-selective Hydrogenation with Thermodynamic Stereocontrol. *J. Am. Chem. Soc.* **2014**, *136*, 1300–1303. (t) George, D. T.; Kuenstner, E. J.; Pronin, S. V. A Concise Approach to Paxilline Indole Diterpenes. *J. Am. Chem. Soc.* **2015**, *137*, 15410–15413. (u) Zhu, K.; Shaver, M. P.; Thomas, S. P. Amine-bis(phenolate) Iron(III)-Catalyzed Formal Hydroamination of Olefins. *Chem.–Asian J.* **2016**, *11*, 977–980. (v) Zheng, J.; Qi, J.; Cui, S. Fe-Catalyzed Olefin Hydroamination with Diazo Compounds for Hydrazone Synthesis. *Org. Lett.* **2016**, *18*, 128–131. (w) Wu, X.; Gannett, C. N.; Liu, J.; Zeng, R.; Novaes, L. F. T.; Wang, H.; Abruña, H. D.; Lin, S. Intercepting Hydrogen Evolution with Hydrogen-Atom Transfer: Electron-Initiated Hydrofunctionalization of Alkenes. *J. Am. Chem. Soc.* **2022**, *144*, 17783–17791.

(19) For seminal examples of MHAT-enabled cross-coupling reactions using transition metals and traditional coupling partners, see: (a) Green, S. A.; Matos, J. L.; Yagi, A.; Shenvi, R. A. Branch-Selective Hydroarylation: Iodoarene-Olefin Cross-Coupling. *J. Am. Chem. Soc.* **2016**, *138*, 12779–12782. (b) Green, S. A.; Vasquez-Céspedes, S.; Shenvi, R. A. Iron-Nickel Dual-Catalysis: A New Engine for Olefin Functionalization and the Formation of Quaternary Centers. *J. Am. Chem. Soc.* **2018**, *140*, 11317–11324. (c) Green, S. A.; Huffman, T. R.; McCourt, R. O.; van der Puyl, V.; Shenvi, R. A. Hydroalkylation of Olefins To Form Quaternary Carbons. *J. Am. Chem. Soc.* **2019**, *141*, 7709–7714.

(20) For recently disclosed or ongoing developments in MHAT cross-couplings that utilize Fe-mediated, outer-sphere bond formation



between radicals, see: (a) Gan, X.-C.; Kotesova, S.; Castanedo, A.; Green, S. A.; Möller, S. L. B.; Shenvi, R. A. Iron-Catalyzed Hydrobenzylation: Stereoselective Synthesis of (–)-Eugenical C. *J. Am. Chem. Soc.* **2023**, *145*, 15714–15720. (b) Kong, L.; Gan, X.-C.; van der Puyl Lovett, V. A.; Shenvi, R. A. Alkene Hydrobenzylation by a Single Catalyst That Mediates Iterative Outer-Sphere Steps. *J. Am. Chem. Soc.* **2024**, *146*, 2351–2357. (c) Gan, X.-C.; Zhang, B.; Dao, N.; Bi, C.; Pokle, M.; Kan, L.; Collins, M. R.; Tyrol, C. C.; Bolduc, P. N.; Nicasstri, M.; Kawamata, Y.; Baran, P. S.; Shenvi, R. A. Carbon Quaternization of Redox Active Esters and Olefins via Decarboxylative Coupling. *ChemRxiv* **2023**, DOI: 10.26434/chemrxiv-2023-7vb8x-v2 (accessed 2024-02-08).

(21) Yuan, M.; Song, Z.; Badir, S. O.; Molander, G. A.; Gutierrez, O. On the Nature of C(sp<sup>3</sup>)-C(sp<sup>2</sup>) Bond Formation in Nickel-Catalyzed Tertiary Radical Cross-Couplings: A Case Study of Ni/Photoredox Catalytic Cross-Coupling of Alkyl Radicals and Aryl Halides. *J. Am. Chem. Soc.* **2020**, *142*, 7225–7234.

(22) Xue, W.; Jia, X.; Wang, X.; Tao, X.; Yin, Z.; Gong, H. Nickel-Catalyzed Formation of Quaternary Carbon Centers Using Tertiary Alkyl Electrophiles. *Chem. Soc. Rev.* **2021**, *50*, 4162–4184.

(23) Liu, W.; Lavagnino, M. N.; Gould, C. A.; Alcázar, J.; MacMillan, D. W. C. A Biomimetic S<sub>H</sub>2 Cross-Coupling Mechanism for Quaternary sp<sup>3</sup>-Carbon Formation. *Science* **2021**, *374*, 1258–1263.

(24) (a) Bour, J. R.; Ferguson, D. M.; McClain, E. J.; Kampf, J. W.; Sanford, M. S. Connecting Organometallic Ni(III) and Ni(IV): Reactions of Carbon-Centered Radicals with High-Valent Organonickel Complexes. *J. Am. Chem. Soc.* **2019**, *141*, 8914–8920. (b) Tsybal, A. V.; Bizzini, L. D.; MacMillan, D. W. C. Nickel Catalysis via S<sub>H</sub>2 Homolytic Substitution: The Double Decarboxylative Cross-Coupling of Aliphatic Acids. *J. Am. Chem. Soc.* **2022**, *144*, 21278–21286. (c) Mao, E.; MacMillan, D. W. C. Late-Stage C(sp<sup>3</sup>)-H Methylation of Drug Molecules. *J. Am. Chem. Soc.* **2023**, *145*, 2787–2793.

(25) For additional discussions regarding bimolecular homolytic substitution and radical sorting in organic/organometallic chemistry, see: (a) Ingold, K. U.; Roberts, B. P. *Free-Radical Substitution Reactions. Bimolecular Homolytic Substitutions (S<sub>H</sub>2 Reactions) at Saturated Multivalent Atoms*, 1st ed.; John Wiley & Sons Inc.: 1971. (b) Johnson, M. D. Bimolecular Homolytic Displacement of Transition-Metal Complexes from Carbon. *Acc. Chem. Res.* **1983**, *16*, 343–349. (c) Halpern, J. Mechanisms of Coenzyme B<sub>12</sub>-Dependent Rearrangements. *Science* **1985**, *227*, 869–875. (d) Walton, J. C. Homolytic Substitution: A Molecular Ménage à Trois. *Acc. Chem. Res.* **1998**, *31*, 99–107. (e) Zhang, Q.; van der Donk, W. A.; Liu, W. Radical-Mediated Enzymatic Methylation: A Tale of Two SAMs. *Acc. Chem. Res.* **2012**, *45*, 555–564.

(26) (a) De Vleeschouwer, F.; Van Speybroeck, V.; Waroquier, M.; Geerlings, P.; De Proft, F. Electrophilicity and Nucleophilicity Index for Radicals. *Org. Lett.* **2007**, *9*, 2721–2724. (b) Parsaee, F.; Senarathna, M. C.; Kannangara, P. B.; Alexander, S. N.; Arche, P. D. E.; Welin, E. R. Radical Philicity and Its Role in Selective Organic Transformations. *Nat. Rev. Chem.* **2021**, *5*, 486–499.

(27) (a) Fischer, H. The Persistent Radical Effect: A Principle for Selective Radical Reactions and Living Radical Polymerizations. *Chem. Rev.* **2001**, *101*, 3581–3610. (b) Leifert, D.; Studer, A. The Persistent Radical Effect in Organic Synthesis. *Angew. Chem., Int. Ed.* **2020**, *59*, 74–108.

(28) Lowry, M. S.; Goldsmith, J. I.; Slinker, J. D.; Rohl, R.; Pascal, R. A.; Malliaras, G. G.; Bernhard, S. Single-Layer Electroluminescent Devices and Photoinduced Hydrogen Production from an Ionic Iridium(III) Complex. *Chem. Mater.* **2005**, *17*, 5712–5719.

(29) (a) Zhang, G.; Bian, C.; Lei, A. Advances in Visible Light-Mediated Oxidative Coupling Reactions. *Chin. J. Catal.* **2015**, *36*, 1428–1439. (b) Reed, N. L.; Yoon, T. P. Oxidase Reactions in Photoredox Catalysis. *Chem. Soc. Rev.* **2021**, *50*, 2954–2967.

(30) For relevant insight into the feasibility of Mn(II)/Mn(III) redox steps under photoredox electron-transfer conditions, see: (a) Yamaguchi, K. S.; Sawyer, D. T. The Redox Chemistry of Manganese(III) and – (IV) Complexes. *Isr. J. Chem.* **1985**, *25*, 164–176. (b) Fu, N.;

Sauer, G. S.; Saha, A.; Loo, A.; Lin, S. Metal-Catalyzed Electrochemical Diazidation of Alkenes. *Science* **2017**, *357*, 575–579.

(31) While the plausible mechanism detailed in Figure 2 is consistent with redox properties and reactivity patterns established in prior catalytic reports, alternative mechanistic scenarios cannot be rigorously excluded at this stage. These complex scenarios may involve, among other possibilities, reductive quenching of photocatalyst 3 by Mn(II) MHAT intermediate XIV, oxidative quenching of photocatalyst 3 by exogenous oxidants (i.e., Bz<sub>2</sub>O<sub>2</sub>), or combinations of all pathways described within this manuscript. Although initial mechanistic experiments have been conducted to probe the open-shell nature of this protocol (see SI for details), further elucidation of all operative elementary steps, as well as their respective contributions to the complex paradigm of Ir/Mn/Ni triple catalytic reactivity, will be the focus of subsequent mechanistic studies that may be reported in due course.

(32) (a) Schönherr, H.; Cernak, T. Profound Methyl Effects in Drug Discovery and a Call for New C-H Methylation Reactions. *Angew. Chem., Int. Ed.* **2013**, *52*, 12256–12267. (b) Dao, H. T.; Li, C.; Michaudel, Q.; Maxwell, B. D.; Baran, P. S. Hydromethylation of Unactivated Olefins. *J. Am. Chem. Soc.* **2015**, *137*, 8046–8049. (c) Law, J. A.; Bartfield, N. M.; Frederick, J. H. Site-Specific Alkene Hydromethylation via Protonolysis of Titanacyclobutanes. *Angew. Chem., Int. Ed.* **2021**, *60*, 14360–14364. (d) Dong, Y.; Shin, K.; Mai, B. K.; Liu, P.; Buchwald, S. L. Copper Hydride-Catalyzed Enantioselective Olefin Hydromethylation. *J. Am. Chem. Soc.* **2022**, *144*, 16303–16309.

(33) Le, C. C.; Wismer, M. K.; Shi, Z. C.; Zhang, R.; Conway, D. V.; Li, G.; Vachal, P.; Davies, I. W.; MacMillan, D. W. C. A General Small-Scale Reactor to Enable Standardization and Acceleration of Photocatalytic Reactions. *ACS Cent. Sci.* **2017**, *3*, 647–653.

(34) Given the nonessential (yet modestly beneficial) behavior of KOAc and water within this system, the role of these additives, including their potential interactions with NHC-adducts, hydrosilanes, metal catalysts or other reaction components, will be the subject of further studies. For discussions on the utility of similar additives within deoxygenative or organosilicon-based protocols, see ref 15a and: (a) Denmark, S. E.; Sweis, R. F. Design and Implementation of New, Silicon-Based, Cross-Coupling Reactions: Importance of Silicon-Oxygen Bonds. *Acc. Chem. Res.* **2002**, *35*, 835–846. (b) Nakao, Y.; Hiyama, T. Silicon-Based Cross-Coupling Reaction: An Environmentally Benign Version. *Chem. Soc. Rev.* **2011**, *40*, 4893–4901. (c) Obradors, C.; Martinez, R. M.; Shenvi, R. A. Ph(*i*-PrO)SiH<sub>2</sub>: An Exceptional Reductant for Metal-Catalyzed Hydrogen Atom Transfers. *J. Am. Chem. Soc.* **2016**, *138*, 4962–4971. (d) Liu, R. Y.; Buchwald, S. L. CuH-Catalyzed Olefin Functionalization: From Hydroamination to Carbonyl Addition. *Acc. Chem. Res.* **2020**, *53*, 1229–1243.

(35) (a) Halpern, J. Determination of Transition Metal-Alkyl Bond Dissociation Energies from Kinetic Measurements. *Polyhedron* **1988**, *7*, 1483–1490. (b) Simoes, J. A. M.; Beauchamp, J. L. Transition Metal–Hydrogen and Metal–Carbon Bond Strengths: The Keys to Catalysis. *Chem. Rev.* **1990**, *90*, 629–688.

(36) For representative descriptions of radical rebound occurring with Fe- or Co-based MHAT catalysts, see refs 20b–c and: (a) Shevick, S. L.; Obradors, C.; Shenvi, R. A. Mechanistic Interrogation of Co/Ni-Dual Catalyzed Hydroarylation. *J. Am. Chem. Soc.* **2018**, *140*, 12056–12068. (b) Sun, H. L.; Yang, F.; Ye, W. T.; Wang, J. J.; Zhu, R. Dual Cobalt and Photoredox Catalysis Enabled Intermolecular Oxidative Hydrofunctionalization. *ACS Catal.* **2020**, *10*, 4983–4989. (c) Nakagawa, M.; Matsuki, Y.; Nagao, K.; Ohmiya, H. A Triple Photoredox/Cobalt/Bronsted Acid Catalysis Enabling Markovnikov Hydroalkoxylation of Unactivated Alkenes. *J. Am. Chem. Soc.* **2022**, *144*, 7953–7959. (d) Wilson, C. V.; Kim, D.; Sharma, A.; Hooper, R. X.; Poli, R.; Hoffman, B. M.; Holland, P. L. Cobalt–Carbon Bonding in a Salen-Supported Cobalt(IV) Alkyl Complex Postulated in Oxidative MHAT Catalysis. *J. Am. Chem. Soc.* **2022**, *144*, 10361–10367. (e) Wilson, C. V.; Holland, P. L. Mechanism of Alkene Hydrofunctionalization by Oxidative Cobalt(salen) Catalyzed Hydrogen Atom Transfer. *J. Am. Chem. Soc.* **2024**, *146*, 2685–2700.

(37) An alternative redox pathway has also been considered for this transformation, in which benzoyloxy radicals (formed *in situ* via fragmentation of  $Bz_2O_2$ ) could directly initiate open-shell deoxygenation from NHC–alcohol adducts through SET processes. This pathway should be exergonic when considering the redox potentials of both benzoyloxy radicals ( $E_{1/2}^{red}[\text{PhCO}_2^\bullet/\text{PhCO}_2^-]$  estimated to be  $>+1.5$  V vs SCE in MeCN) and alcohol adducts based on NHC-1 (for methanol-based intermediate II,  $E_{pa}[\text{II}/\text{II}^{*+}] = +0.99$  V vs SCE in MeCN). Moreover, the *in situ* formation of benzoyloxy radicals has been previously observed when subjecting peroxides to direct photolysis under blue light irradiation. However, this photolysis procedure is reportedly inefficient when compared to protocols involving Ir photosensitizers, consistent with the observation of only 19% product yield in the absence of photocatalyst (Table 1, entry 11). Based on these considerations, we hypothesize that benzoyloxy radical-mediated alcohol activation could contribute as a minor pathway in this reaction, but we instead favor the plausible redox mechanism outlined in Figure 2 as the major route for product formation. For additional details related to the potential benzoyloxy radical-mediated sequence described above, see ref 15a and: (a) Chandross, E. A.; Sonntag, F. I. Chemiluminescent Electron-Transfer Reactions of Radical Anions. *J. Am. Chem. Soc.* **1966**, *88*, 1089–1096. (b) Vasilopoulos, A.; Krska, S. W.; Stahl, S. S. C(sp<sup>3</sup>)–H Methylation Enabled by Peroxide Photosensitization and Ni-Mediated Radical Coupling. *Science* **2021**, *372*, 398–403.

(38) For additional details related to reaction optimization, as well as evidence for open-shell reactivity consistent with the plausible mechanism shown in Figure 2, see SI and Tables S1–S11.

(39) (a) Diccianni, J. B.; Diao, T. Mechanisms of Nickel-Catalyzed Cross-Coupling Reactions. *Trends Chem.* **2019**, *1*, 830–844. (b) Greaves, M. E.; Johnson Humphrey, E. L. B.; Nelson, D. J. Reactions of Ni(0) with Organochlorides, Organobromides, and Organoiodides: Mechanisms and Structure/Activity Relationships. *Catal. Sci. Technol.* **2021**, *11*, 2980–2996.

(40) El-Maiss, J.; El Dine, T. M.; Lu, C.-S.; Karamé, I.; Kanj, A.; Polychronopoulou, K.; Shaya, J. Recent Advances in Metal-Catalyzed Alkyl-Boron (C(sp<sup>3</sup>)-C(sp<sup>2</sup>)) Suzuki-Miyaura Cross-Couplings. *Catalysts* **2020**, *10*, 296.

(41) For more details on high-value aliphatic scaffolds in medicinal chemistry contexts, see: (a) Lovering, F. Escape from Flatland 2: Complexity and Promiscuity. *MedChemComm* **2013**, *4*, 515–519. (b) Talele, T. T. Natural-Products-Inspired Use of the gem-Dimethyl Group in Medicinal Chemistry. *J. Med. Chem.* **2018**, *61*, 2166–2210. (c) Piotrowski, D. W.; Futatsugi, K.; Casimiro-Garcia, A.; Wei, L.; Sammons, M. F.; Herr, M.; Jiao, W.; Lavergne, S. Y.; Coffey, S. B.; Wright, S. W.; et al. Identification of Morpholino-2H-Pyrido[3,2-b][1,4]Oxazin-3(4H)-Ones as Nonsteroidal Mineralocorticoid Antagonists. *J. Med. Chem.* **2018**, *61*, 1086–1097. (d) Ling, T.; Rivas, F. All-Carbon Quaternary Centers in Natural Products and Medicinal Chemistry: Recent Advances. *Tetrahedron* **2016**, *72*, 6729–6777.

(42) For additional examples of deoxygenative hydromethylation or hydroalkylation (including those displaying tolerance of other activated  $\pi$ -systems and distal functionality such as alkyl bromides, epoxides or allylic phenolates), as well as compiled reactivity trends and supplemental observations regarding substrates which are most effective in this method, see Figures S3–S5.

(43) For representative examples of epoxide lability under traditional Ni cross-coupling conditions, see: (a) Molinaro, C.; Jamison, T. F. Nickel-Catalyzed Reductive Coupling of Alkynes and Epoxides. *J. Am. Chem. Soc.* **2003**, *125*, 8076–8077. (b) Nielsen, D. K.; Doyle, A. G. Nickel-Catalyzed Cross-Coupling of Styrenyl Epoxides with Boronic Acids. *Angew. Chem., Int. Ed.* **2011**, *50*, 6056–6059.

(44) Slagt, V. F.; de Vries, A. H. M.; de Vries, J. G.; Kellogg, R. M. Practical Aspects of Carbon-Carbon Cross-Coupling Reactions Using Heteroarenes. *Org. Process Res. Dev.* **2010**, *14*, 30–47.

(45) Bogdos, M. K.; Müller, P.; Morandi, B. Structural Evidence for Aromatic Heterocycle N–O Bond Activation via Oxidative Addition. *Organometallics* **2023**, *42*, 211–217.